Carbohydrate Polymers 111 (2014) 18–24

Contents lists available at ScienceDirect

Carbohydrate Polymers

journal homepage: www.elsevier.com/locate/carbpol

Controlled release of liposome-encapsulated Naproxen from core-sheath electrospun nanofibers

Zhuang Li[a,b], Hongliang Kang[a], Ning Che[a,b], Zhijing Liu[a,b], Pingping Li[a,b], Weiwei Li[a], Chao Zhang[a,b], Chun Cao[a,b], Ruigang Liu[a,*], Yong Huang[a,c,**]

[a] State Key Laboratory of Polymer Physics and Chemistry, Beijing National Laboratory of Molecular Sciences, Institute of Chemistry, Chinese Academy of Sciences, Beijing 100190, China
[b] University of Chinese Academy of Science, Beijing 100049, China
[c] National Research Center for Engineering Plastics, Technical Institute of Physics & Chemistry, Chinese Academy of Sciences, Beijing 100190, China

ARTICLE INFO

Article history:
Received 19 January 2014
Received in revised form 9 April 2014
Accepted 9 April 2014
Available online 18 April 2014

Keywords:
Core-sheath nanofibers
Electrospinning
Cellulose acetate
Liposomes
Naproxen
Sustained drug release

ABSTRACT

Naproxen (NAP) loaded nanofibers of different structures have been successfully prepared by electrospinning. The structures of the nanofibers are NAP and cellulose acetate (CA) mixed nanofibers (NF-1), nanofibers with NAP/CA mixed core and CA sheath (NF-2), and NAP loaded liposomes and sodium hyaluronate (HA-Na) mixed core with CA sheath (NF-3). The structure and morphology of the nanofibers were characterized and the drug release behaviors were investigated. It was found that NAP can disperse in the HA-Na or CA matrix in molecular level without formation of NAP crystals and dimers. The drug release behaviors of NF-1 and NF-2 show a non-Fickian diffusion mechanism, while the NF-3 shows a specific drug release behavior with a burst release within 8 h followed by a sustained drug release for 12 days. The particular two-stage drug release behavior of NF-3 nanofibers offers the materials promising applications as wound dressing materials.

© 2014 Elsevier Ltd. All rights reserved.

1. Introduction

Nanofibers have been extensively studied as tissue engineering scaffolds for decades. Owing to high specific surface area ratio and high porosity, drug-loaded electrospun nanofibers have found clinical applications in wound dressings, orthopedics and tissue regeneration (Holzapfel et al., 2013; Liu et al., 2012; Schiffman & Schauer, 2008). The development of electrospinning techniques has brought forward multiple approaches to fabricate various nanofibers from synthetic and natural polymers (Gupta, Elkins, Long, & Wilkes, 2005; Ohkawa, Minato, Kumagai, Hayashi, & Yamamoto, 2006; Zhang & Chang, 2008). Bio-friendly nanofibers loading various drugs and bioactive molecules thus are widely studied as drug delivery systems (Buschle-Diller et al., 2007; Xie et al., 2013). Among the challenges for nanofiber drug carriers, the most important one is to control the burst drug release. The burst drug release is helpful to suppress the infection and pain of a wound during the initial stage. However, sustained drug release is more important for efficiently protecting the wound for long periods without changing the wound dressing, which is good for wound healing and alleviates the pain caused by dressing changes.

Nanofibers produced by directly electrospinning from drug/polymer mixed solution have drugs dispersed in the polymer matrix, which usually display burst drug release behaviors via Fickian or non-Fickian diffusion (Tungprapa, Jangchud, & Supaphol, 2007; Yu, Yu, Chen, Williams, & Wang, 2012b). Various approaches have been tried to control the burst drug release from nanofiber mats, among which coaxial electrospinning has proved to be an effective one. In the coaxial electrospinning approach, core-sheath nanofibers with drugs embedded in the core matrix can be produced. It was reported that ketoprofen-loaded cellulose acetate (CA) fibers coated with blank CA sheath have no burst release and can provide a zero-order in vitro drug release profile over 96 h (Yu, Yang, Li, Lu, & Zhu, 2012a). Sustained drug release from electrospun nanofibers can also be achieved by encapsulating drug-loaded vehicles in the electrospun nanofibers (Qi et al., 2010; Shao et al., 2011; Song, Wu, & Chang, 2012). It was found that burst release of protein can be avoided by embedding protein-loaded

* Corresponding author. Tel.: +86 10 82618573; fax: +86 10 82618573.
** Corresponding author at: State Key Laboratory of Polymer Physics and Chemistry, Beijing National Laboratory of Molecular Sciences, Institute of Chemistry, Chinese Academy of Sciences, Beijing 100190, China. Tel.: +86 10 82618573; fax: +86 10 82618573.
E-mail addresses: rgliu@iccas.ac.cn (R. Liu), yhuang@mail.ipc.ac.cn (Y. Huang).

http://dx.doi.org/10.1016/j.carbpol.2014.04.017
0144-8617/© 2014 Elsevier Ltd. All rights reserved.

liposomes in the core matrix of core-sheath nanofibers (Mickova et al., 2012). The incorporation of drug-loaded (nano)particles into electrospun fibers can also efficiently prolong the drug release time. (Coneski, Nash, & Schoenfisch, 2011; Hou et al., 2013; Koh, Carpenter, Slomberg, & Schoenfisch, 2013; Xie et al., 2013).

Desired drug-loaded wound dressings should have a burst drug release at the beginning and then a sustained drug release for a long period. However, no such dressings has been prepared. In this work, CA and HA-Na were used to prepare core-sheath nanofibers with the CA sheath and HA-Na core by coaxial electrospinning. Due to that HA-Na can stabilize liposomes by adsorbing on the surfaces (Quemeneur, Rinaudo, Maret, & Pepin-Donat, 2010), Naproxen (NAP) loaded liposomes were embedded in the HA-Na core of the nanofibers. The morphology and drug release behavior of the nanofibers were investigated and were compared with nanofibers of different structures. It was found that the approach in present work could successfully prepare nanofibers that have a burst drug release at the initial stage and subsequently a sustained drug release for a long period.

2. Experimental

2.1. Materials

Cellulose acetate (CA, M_r = 29 kDa, DS = 2.4–2.5) was purchased from Sigma Aldrich (USA). Lecithin (PC, from Soybean) and sodium hyaluronate (HA-Na, $M_w > 10^3$ kDa) were supplied by Aladdin (China). Cholesterol (Chol) and naproxen (NAP) were purchased from Alfa Aesar (USA). Highly purified water was prepared using Milli-Q Water Purification System (Millipore, USA). Dimethyl sulfoxide (DMSO) was supplied by Beijing chemical Works and distilled before use. Other chemicals including chloroform, methanol, acetone and *N*,*N*-dimethylacetamide (DMAc) are all analytical grade and were used as received.

2.2. Preparation of NAP loaded liposomes

NAP loaded liposomes were prepared from PC, Chol and NAP using the conventional thin film hydration method. Briefly, 160 mg PC, 20 mg Chol and 90 mg NAP were added to a 250 mL round bottom flask and then were dissolved in 5 mL mixed solvent of chloroform and methanol (2:1, v/v). Thin lipid film was produced by evaporating the solvents using a rotary evaporator operated at 30 °C and 60 rpm. The dried lipid film was then hydrated with 5 mL water using the above conditions in a nitrogen atmosphere. After being swollen overnight, the dispersion was sonicated in an ultrasonic water bath for 1 h at room temperature to generate narrowly distributed NAP loaded liposomes. The resultant NAP loaded liposomes are in the size of intermediate-size unilamellar vesicles (IUVs) and are denoted as NAP-IUVs henceforce.

The encapsulation efficiency of NAP in the liposomes was defined by Q_w (%) = $W_e/W_N \times 100$, where W_e and W_N are the mass of NAP encapsulated in the liposomes and the amount of NAP used during the preparation of NAP-IUVs. To determine Q_w (%), the as-prepared NAP-IUVs dispersion was centrifuged 10 min at 10^4 rpm to remove the un-encapsulated NAP, which is normally precipitated in aqueous solution. The supernatant was lyophilized and weighed to obtain the mass (W_s) of the NAP loaded liposomes. The mass of the encapsulated NAP was determined as follows. The lyophilized sample was first dissolved in 2 mL DMSO and then diluted to 100 mL by buffer solution (pH = 6.4). The concentration of NAP (C_N) in the resultant solution was determined by comparing the UV absorbance at wavelength of 262 nm to a calibration curve of UV absorbance intensity versus NAP concentration, by which the mass of the encapsulated NAP (W_e) in the samples was determined. The corresponding feeding mass of NAP (W_N) is half to that of pure liposomes, which can be calculated by $(W_s - 100C_N)/2$.

2.3. Preparation of NAP loaded nanofibers

Core-sheath nanofibers with CA sheath and HA-Na core were prepared as follows. NAP-IUVs-HA-Na aqueous solution and CA (17%, w/v) solution in acetone/DMAc (2:1, v/v) were used as the core and sheath fluids of coaxial electrospinning, respectively. The core fluid was prepared in advance by mixing NAP-IUVs dispersion with HA-Na aqueous solution (3%, w/v) in a bottle in the volume ratio of 1:2 using a vortex shaker. The needle was settled coaxially by two needles with inner diameters of 0.5 and 1.2 mm. Extruding rates were set at 0.05 and 0.37 mL/h for the core and sheath solutions, respectively. The voltage and the distance between the needle and the collector (aluminum foil) were set at 15 kV and 15 cm, respectively. The electrospinning was carried out at room temperature and a humidity of about 20%. The resultant nanofibers were denoted as NF-3.

For comparison, NAP loaded CA nanofibers were also prepared from NAP/CA (1.9%/19%, w/v) mixed solution in acetone/DMAc (2:1, v/v). The needle used has a inner diameter of 1.0 mm and the extruding rate was 0.5 mL/h. The electrospinning was operated at 12 kV with needle to collector distance of 15 cm. The resulted nanofibers were denoted as NF-1. Core-sheath nanofibers with CA sheath and NAP/CA core were prepared by coaxial electrospinning. The CA (19%, w/v) and NAP/CA (1.9%/19%, w/v) solutions were used as the sheath and core fluids, respectively. Coaxially settled needles with inner diameter of 0.7 and 1.4 mm were used and the fluid extruding rates were both 0.5 mL/h. The electrospinning was operated at 15 kV with needle to collector distance of 15 cm. The prepared core-sheath nanofibers were denoted as NF-2. The two coaxial needles used were different, because they were selected depending on the properties of the respective fluids to avoid plugging and to prepare desired nanofibers.

NAP content in the nanofibers was determined by UV absorbance. About 350 mg nanofibers (W_1) was dissolved in 2 mL DMSO. The solution was then diluted to 100 mL with buffer solution (pH = 6.4) that was prepared by dissolving potassium dihydrogen phosphate and sodium hydroxide in water. The concentration of NAP (C_N) in the resultant solution was determined by UV absorbance as described above, by which the mass of NAP in the nanofibers (W_N) was determined. The content of NAP in the nanofibers was calculated by C (%) = $W_N/W_1 \times 100$.

2.4. Instruments and characterization

The morphology of the electrospun fibers was observed on a field emission scanning electron microscope (FESEM, JEOL 6700, Japan) operated at accelerating voltage of 5 kV and current of 10 μA. The samples on aluminum foil were sputter-coated with a layer of platinum using a sputter-coater (BAL-TEC, SCD 500, Switzerland) before observation. All the images were taken in secondary electron mode. Elemental analysis was performed on an energy dispersive X-ray spectrometer (EDS, Oxford, UK). Transmission electron microscope (TEM) observation of the nanofibers was carried out on a field emission transmission electron microscopy (FETEM, 2200FS, JEOL, Japan). The samples were prepared by fixing copper grids on the collector and collecting fibers during the electrospinning. The operation voltage of TEM was set 200 kV, and the images were recorded in bright field mode.

Differential scanning calorimetry (DSC) measurements were carried out on DSC Q2000 (TA Instruments, USA) in the range of 20–200 °C at the heating rate of 10 °C/min in a nitrogen atmosphere. Wide angle X-ray diffraction (WAXD) experiments were carried out on a D/max 2500 X-ray diffraction meter (Rigaku, Japan).

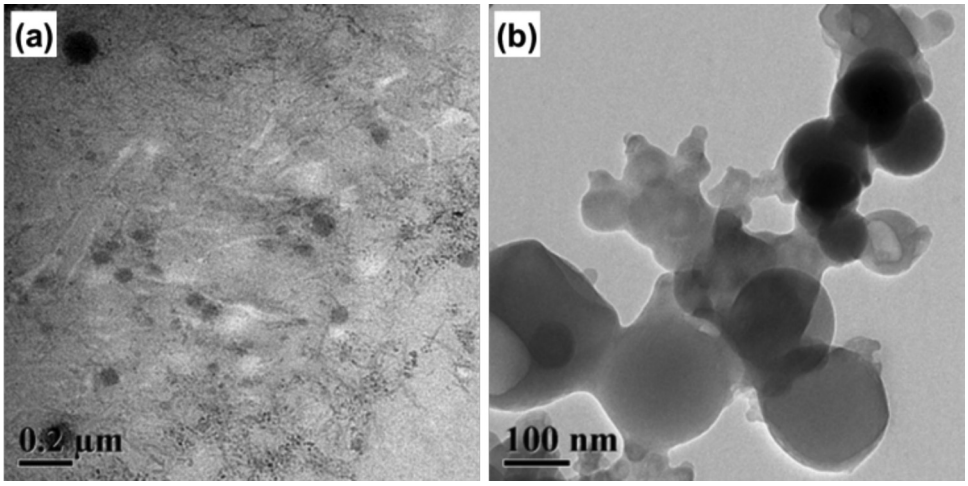

Fig. 1. Typical TEM images of NAP loaded liposomes (a) and the enlarged image (b).

CuK_α X-ray (λ = 0.154 nm) was used as the radiation source. Operation parameters were set at 40 kV and 200 mA and the data in the range of 2θ = 5–60° were recorded. Fourier transform infrared spectroscopy (FTIR, EQUINOX55, Bruker, Germany) was used to characterize the fiber mats in a range of 400–4000 cm^{-1} and a resolution of 2 cm^{-1}. Absorbance of NAP at 262 nm was measured on a UV–vis spectrophotometer (TU-1901, Purkinje General, China) and compared with the calibration curve of UV absorbance to a series of NAP concentrations to obtain the NAP concentration in the buffer solutions.

2.5. In vitro drug release

The in vitro drug release experiments of the NAP loaded nanofibers were carried out as follows. NAP loaded nanofibers were placed in a dialysis bag with molecular weight cutoff of 3.50 kDa. The dialysis bag was then immersed in a buffer solution (pH = 6.4) with desired volume. The temperature of the buffer solution was set at 37 ± 0.5 °C to mimic the physiological conditions of human skin (pH around 5.0–6.5). The buffer solution was stirred continuously at 200 rpm and the NAP concentration in the buffer solution was determined at desired time by UV–vis absorbance. In the measurement, 2 mL buffer solution was withdrawn and replaced by 2 mL fresh buffer solution each time to maintain a constant volume.

The accumulative release of NAP from the nanofibers (P%) was calculated using the following equation (Locock et al., 2013),

$$P(\%) = \frac{C_n \times V_0 + \sum_{i=1}^{n-1} C_t \times V}{W_0} \quad (1)$$

where C_n is the NAP concentration determined at No. n and C_i is the NAP concentration determined at No. i, V_0 is the volume of the buffer and V is the volume of the withdrawn sample, W_0 is the total amount of NAP in the fibers. Three parallel experiments were carried out and the mean value was plotted as a function of time.

3. Results and discussion

3.1. Preparation of NAP loaded nanofibers

Liposomes are self-assembled bilayer phospholipid vesicles, which can be used as carriers of both hydrophilic and hydrophobic cargos. As the cargos release slowly due to lower mass transfer coefficient (Mourtas et al., 2007; Pjanovic et al., 2010), liposomes can be used as drug delivery vehicles for sustained release (Allen & Cullis, 2013; Bochot & Fattal, 2012). Naproxen (NAP) is a non-steroidal anti-inflammatory drug and is commonly used to treat the inflammation and pain of various wounds. In case of encapsulating NAP in liposomes, NAP is generally located between the bilayer membranes due to its hydrophobicity (Puglia et al., 2010). In our work, NAP loaded liposomes were prepared to control the NAP release of the electrospun nanofibers. Fig. 1 shows the TEM images of the NAP loaded liposomes. It indicates that the diameter of the liposomes is in the range of 50–150 nm, which are generally intermediate-size unilamellar vesicles (IUVs). The encapsulation efficiency test indicates that about 26.4 wt.% of the fed NAP was encapsulated in the prepared liposomes. The low encapsulation efficiency may be attributed to the relatively small partition coefficient of NAP ($\log P$ = 3.22) (Puglia et al., 2010).

HA-Na can stabilize liposomes by absorbing on their surfaces (Quemeneur et al., 2010). Therefore, an aqueous mixture of HA-Na and NAP-IUVs was used as the core fluid while CA solution in acetone/DMAc mixed solvent was used as the sheath fluid in coaxial electrospinning. The obtained core-sheath nanofibers (NF-3) have smooth surfaces with average diameter of 359.4 ± 126.2 nm (Fig. 2). EDS results indicate that only carbon and oxygen elements can be detected on the surface of the ultrathin fibers of different diameters in the depth of 5–10 nm. The nitrogen and sodium elements from HA-Na, and the phosphorus element from PC do not appear in EDS spectra of the nanofibers, confirming that no fluids mixing occurred and the embedded liposomes were not ruptured during the electrospinning. The Al signal in the spectrum comes from the aluminum foil, which was used as the collector of the nanofibers.

Fig. 3 shows the TEM images of the liposome-loaded nanofibers. The results confirm that the resultant nanofibers have the typical core-sheath structure with the sheath thickness of about 20–50 nm. The loaded liposomes are difficult be observed in TEM images due to limited contrast between liposomes and HA-Na.

For comparison, NF-1 and NF-2 nanofibers were also prepared. The SEM images and the corresponding average diameters are shown Fig. S1. The results indicate that both nanofibers have smooth surfaces with an average diameter about 410 nm. Moreover, TEM observation indicates that the NF-1 nanofibers are uniform, confirming that NAP molecules are dispersed homogeneously in the CA matrix (Fig. S2a). While the NF-2 nanofibers clearly have a core-sheath structure, which comes from the different composition of the CA sheath and the NAP/CA core matrix.

3.2. Dispersion of NAP in polymeric matrix

Solubility of hydrophobic drugs such as NAP is quite important for improvement of the drug efficiency, which can be achieved by

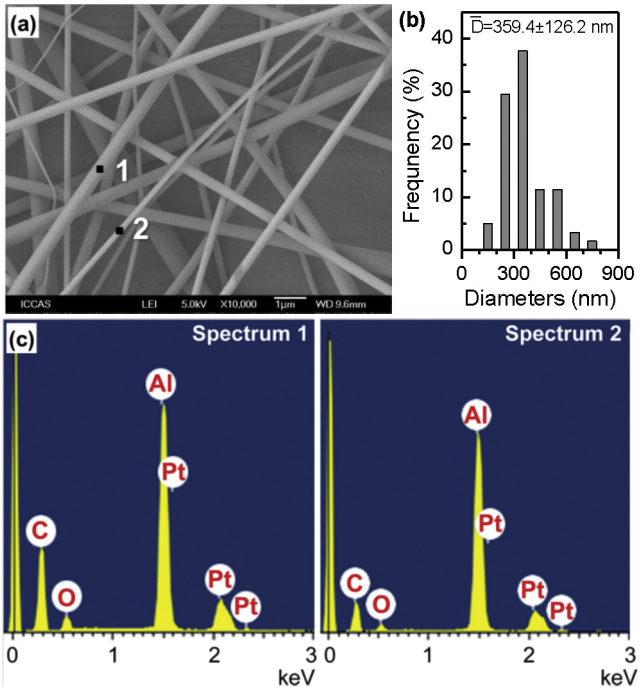

Fig. 2. Typical (a) SEM image and (b) corresponding diameter distribution and (c) EDS results of NF-3 nanofibers. Spectra 1 and 2 correspond to the points 1 and 2 indicated in (a), respectively.

adding additives to reduce the crystallinity of the drugs. Fig. 4a b shows the DSC and XRD results of the NAP loaded nanofibers. The results of NAP, CA and HA-Na are also provided for comparison. On the DSC curves, there is no melting peak of NAP crystals, which indicates that no NAP crystal formed in the nanofibers. XRD results further confirmed that no NAP crystals exist in the nanofibers. These results are consistent with the TEM observations (Figs. 3 and S2), in which no NAP crystals can be observed.

For the clarification of the interactions between NAP and the polymeric matrix, FTIR experiments were carried out and the results are shown in Fig. 4c. The well-defined sharp absorption peak of pure NAP is at 1728 cm^{-1}, which comes from the stretching vibration of the carbonyl groups. The absorption peak of carbonyl groups of pure CA locates at 1753 cm^{-1}. For NAP loaded nanofibers (NF-1, NF-2, and NF-3), the absorption peak of carbonyl groups shifts to 1743 cm^{-1}, indicating that there are interactions between the carbonyl groups of NAP and CA molecules. Moreover, the strong broad absorption peak of the hydroxyl group of NAP dimers in pure NAP at around 3150 cm^{-1} disappeared on the FTIR spectra of the NAP loaded nanofibers. Meanwhile, the absorption peak from the –OH groups of CA at around 3520 cm^{-1} red shifted to around 3470 cm^{-1} on FTIR spectra of NAP loaded nanofibers. FTIR results suggested that the hydrogen bonds of NAP dimers were replaced by the hydrogen bonds between NAP and CA molecules as indicated in Fig. 5, which resulted in the molecular level dispersion of NAP in CA matrix of the nanofibers. The spectrum of the NF-3 nanofiber mats is similar to those of NF-1 and NF-2 nanofibers, which may result from similar interactions between NAP and HA-Na molecules. These results confirm that the hydrogen bonding interactions between NAP and CA or HA-Na molecules can efficiently prevent the crystallization of NAP and enhance the solubility of NAP in the nanofibers.

Table 1
NAP content and parameters of the nanofibers.

Sample	NAP content (wt.%)		Nanofiber diameter (nm)
	Feeding	Actual	
NF-1	9.09	9.39	409.3 ± 152.5
NF-2	4.76	4.72	419.2 ± 178.2
NF-3	0.49	0.48	359.4 ± 126.2

3.3. *In vitro drug release of the nanofibers*

NAP content of the prepared nanofibers is listed in Table 1. The results indicate that the content of the NAP in the nanofibers is similar to the feeding values. The in vitro NAP release profiles of the nanofibers are shown in Fig. 6. Results and standard deviations are the result of three parallel experiments. The results show that NF-1 and NF-2 nanofibers have the similar drug release profiles. The slower drug release rate of NF-2 nanofibers is due to the CA sheath, which postpones the diffusion of NAP out of the nanofibers. Moreover, the average diameter of the NF-2 nanofibers is slightly larger than that of NF-1 nanofibers, which could also contribute to the slower release of the loaded NAP.

Compared with those of NF-1 and NF-2 nanofibers, the drug release profile of NF-3 nanofibers is quite different. Obviously, the drug release of NF-3 can be divided into two stages. In the first stage, the loaded NAP released relatively quickly, with about 47.1% of NAP was released from the nanofibers within 8 h. In the second stage, the release of the left NAP was relatively slow and was sustained for

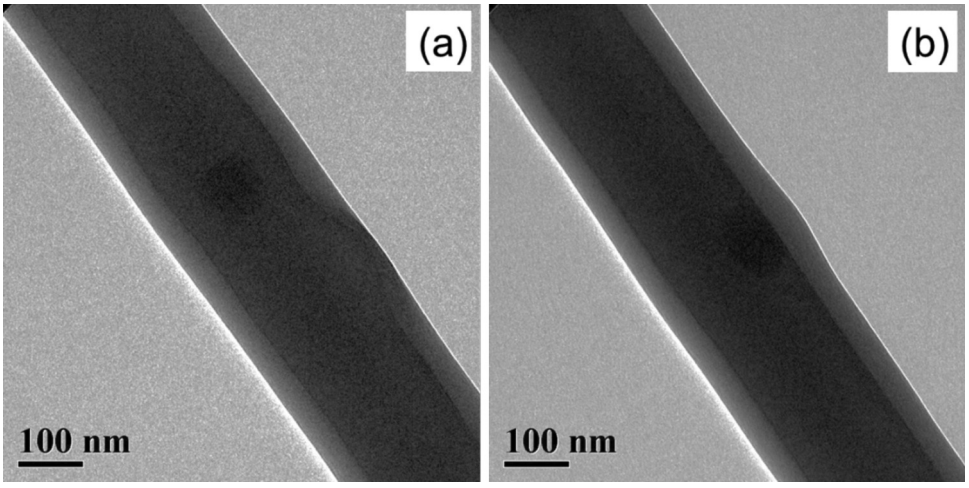

Fig. 3. Typical TEM images of NF-3 nanofibers with liposomes located at the (a) middle and (b) aside of the core matrix indicated in the circles.

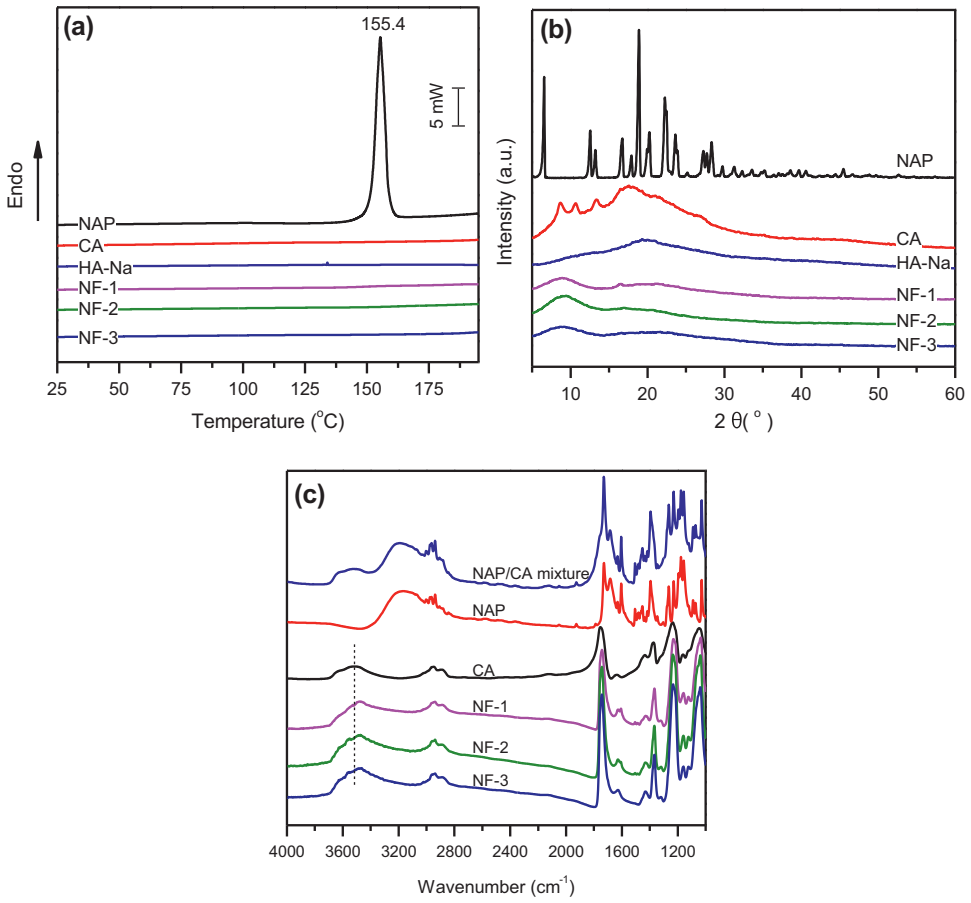

Fig. 4. DSC traces (a) and XRD curves (b) and FTIR spectra (c) of the NAP loaded nanofibers and correlated raw materials.

about 12 days (Fig. 6b). The two-stage release behavior could be due to that NAP was directly dispersed in the core HA-Na matrix besides that which was encapsulated in liposomes. According to the measured encapsulation efficiency of NAP in liposomes, about 73.6% of the feeding NAP was located outside of the liposomes in the core HANa matrix. The un-encapsulated NAP can be released rapidly by diffusing out of the CA sheath, which is similar to the release of NAP from the NF-2 nanofibers. Comparing the fast release step of NF-3 nanofibers with those of NF-1 and NF-2 nanofibers, only 64.0% of the unencapsulated NAP in NF-3 diffused out during the first stage, which is much lower than those of NF-1 (90.9%) and NF-2 (80.3%) nanofibers. The slower NAP release from NF-3 nanofibers is due to the relatively strong interaction between HA-Na and NAP. For the liposome-encapsulated NAP in the NF-3 nanofibers, the NAP first diffused out through the liposome membrane and then the CA sheath of the core-sheath nanofibers. It has been reported that the mass transfer coefficient of the liposome-encapsulated drugs is quite low (Mourtas et al., 2007; Pjanovic et al., 2010). Therefore, the slow NAP release from the NF-3 nanofibers during the second stage mainly results from the encapsulation of NAP by the liposomes. It should be noted that the diameters of the nanofibers have high standard deviation (Table 1), which could surely influence the drug release behaviors of the nanofibers. However, nanofibers in present work have similar average diameters and distribution.

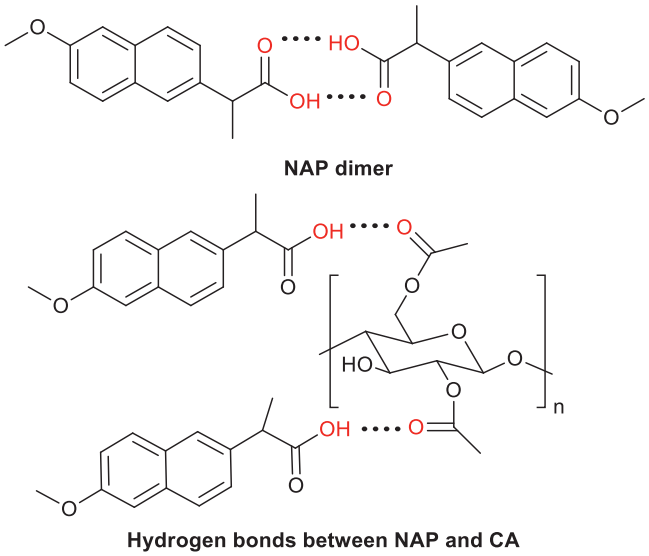

Fig. 5. The hydrogen bonds of NAP dimer and NAP-CA.

The NAP release profiles can be analyzed by using Peppas equation (Peppas & Sahlin, 1989; Ritger & Peppas, 1987a,b)

$$Q = kt^n \quad (2)$$

where Q is the cumulative drug release in percentage, t is the release time in hours, k is a constant reflecting the structural and geometric characteristics of the carriers, and n is the release component that corresponds to the release mechanism of the loaded drugs. The data analysis results are listed in Table 2. The results indicate that the values of n for NF-1 and NF-2 nanofibers are 0.6353 and 0.8442, respectively. Both are in the range of 0.45–0.89, which suggest a typical non-Fickian diffusion caused by the relatively strong interaction between NAP and CA molecules. For NF-3 nanofibers, the n values of the two release stages are different. The value of n in the

Table 2
Data fit parameters of NAP release profiles from nanofibers.

Nanofibers	Linear release parameters		Regressed equation	
	Equation	R^{2*}	Peppas equation	R^2
NF-1	$Q = 10.45t + 12.40$	0.9381[a]	$Q = 20.00t^{0.64}$	0.8521
NF-2	$Q = 9.09t + 7.38$	0.9528[b]	$Q = 11.58t^{0.84}$	0.8718
NF-3	$Q = 5.63t + 3.35$	0.9745[c]	$Q = 6.84t^{0.96}$	0.9775
	$Q = 0.19t + 44.15$	0.9808[d]	$Q = 25.50t^{0.22}$	0.8656

* Correlation coefficient regressed according to the linear release equation before [a]8 h, [b]10 h, [c]8 h, and [d]from 8 h to 336 h.

first stage is close to 1 (0.9696), which suggests a near zero-order drug release behavior. In contrast, for the second stage, the value of n is lower than 0.45 (0.2202), which indicated a Fickian diffusion mechanism in this stage.

The special drug release of NF-3 nanofibers with a burst NAP release followed by a sustained one make it have promising applications in wound dressing materials. Generally, the healing process of an acute wound can be summarized into five consecutive cascades of events, including hemostasis, inflammation, migration, proliferation and maturation (Zahedi, Rezaeian, Ranaei-Siadat, Jafari, & Supaphol, 2010). Hemostasis and inflammation occur soon after damage to the skin. Migration and proliferation last about 2 weeks

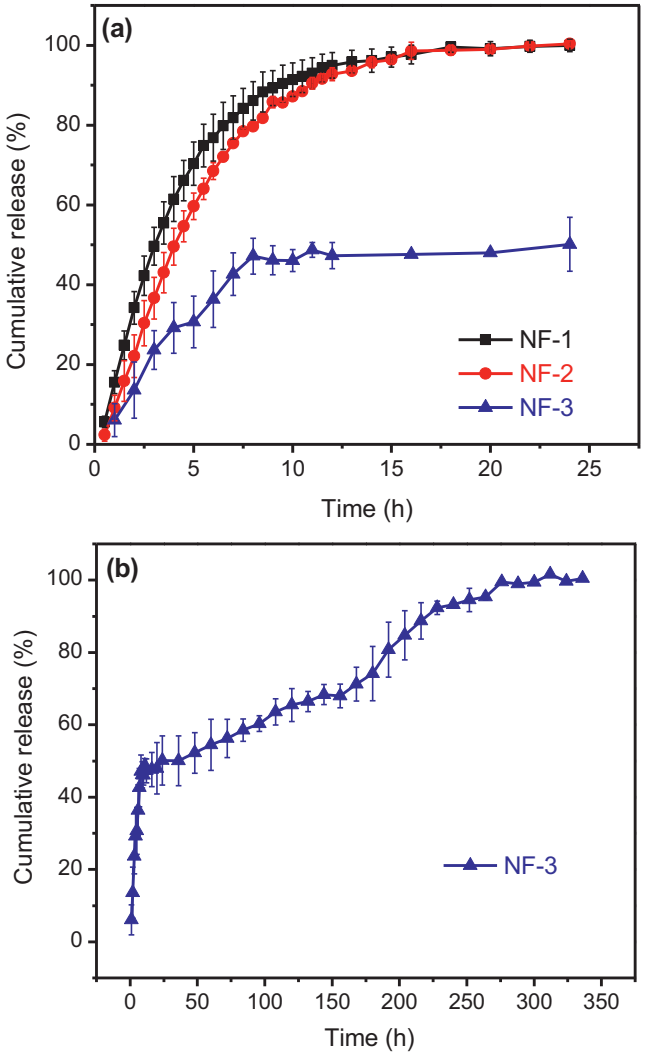

Fig. 6. In vitro NAP release of nanofibers. (a) NAP release profiles in the first 24 h. (b) NAP release profile of NF-3 nanofibers in full range.

while maturation takes in 8–12 weeks. In the case of using NF-3 nanofiber mats as the dressing materials on an acute wound, the burst release of NAP could quickly relieve the pain and protect the wound in time. Meanwhile, the following sustained release could offer a persistent protection until proliferation of the wound was complete. The dressing could work long enough to heal the wound even without a change. On the other hand, compared with the oral administration of NAP with 500 mg in twice-daily dosing and peak plasma concentrations in about 2 h (Capone et al., 2005; Davies & Anderson, 1997; Todd & Clissold, 1990), local administration of NAP from the wound dressing of nanofibers should be more efficient and faster.

4. Conclusions

NAP loaded nanofibers of different structures were successfully prepared by electrospinning. The structures of the nanofibers are NAP and cellulose acetate (CA) mixed nanofibers (NF-1), NAP/CA mixed core with CA sheath (NF-2), and NAP loaded liposomes and sodium hyaluronate (HA-Na) mixed core with CA sheath (NF-3). It was found that NAP can form hydrogen bonds with CA and HA-Na molecules, leading to the homogenous dispersion of NAP in the polymer matrixes of the nanofibers. Drug release from NF-1 and NF-2 nanofibers is by a non-Fickian diffusion mechanism. In contrast, the NF-3 nanofibers show a specific drug release behavior, in which a burst drug release for the first 8 h is followed by a sustained drug release lasting for 12 days. The specific drug release behavior of the NF-3 nanofibers may indicate the promise of these materials for applications in wound dressings.

Acknowledgements

This work was supported by the National Natural Science Foundation of China (Nos. 20974114, 21174150, and 21174156), National Program on Key Basic Research Project of China (973 Program) (No. 2011CB605604), and the Knowledge Innovation Program of the Chinese Academy of Sciences (No. KJCX2-YW-H19).

Appendix A. Supplementary data

Supplementary data associated with this article can be found, in the online version, at http://dx.doi.org/10.1016/j.carbpol.2014.04.017.

References

Allen, T. M., & Cullis, P. R. (2013). Liposomal drug delivery systems: From concept to clinical applications. *Advanced Drug Delivery Reviews*, *65*(1), 36–48.
Bochot, A., & Fattal, E. (2012). Liposomes for intravitreal drug delivery: A state of the art. *Journal of Controlled Release*, *161*(2), 628–634.
Buschle-Diller, G., Cooper, J., Xie, Z. W., Wu, Y., Waldrup, J., & Ren, X. H. (2007). Release of antibiotics from electrospun bicomponent fibers. *Cellulose*, *14*(6), 553–562.
Capone, M. L., Sciulli, M. G., Tacconelli, S., Grana, M., Ricciotti, E., Renda, G., et al. (2005). Pharmacodynamic interaction of naproxen with low-dose aspirin in healthy subjects. *Journal of the American College of Cardiology*, *45*(8), 1295–1301.
Coneski, P. N., Nash, J. A., & Schoenfisch, M. H. (2011). Nitric oxide-releasing electrospun polymer microfibers. *ACS Applied Materials & Interfaces*, *3*(2), 426–432.
Davies, N. M., & Anderson, K. E. (1997). Clinical pharmacokinetics of naproxen. *Clinical Pharmacokinetics*, *32*(4), 268–293.
Gupta, P., Elkins, C., Long, T. E., & Wilkes, G. L. (2005). Electrospinning of linear homopolymers of poly(methyl methacrylate): Exploring relationships between fiber formation, viscosity, molecular weight and concentration in a good solvent. *Polymer*, *46*(13), 4799–4810.
Holzapfel, B. M., Reichert, J. C., Schantz, J.-T., Gbureck, U., Rackwitz, L., Nöth, U., et al. (2013). How smart do biomaterials need to be? A translational science and clinical point of view. *Advanced Drug Delivery Reviews*, *65*(4), 581–603.
Hou, Z., Li, X., Li, C., Dai, Y., Ma, P., Zhang, X., et al. (2013). Electrospun upconversion composite fibers as dual drugs delivery system with individual release properties. *Langmuir*, *29*(30), 9473–9482.

Koh, A., Carpenter, A. W., Slomberg, D. L., & Schoenfisch, M. H. (2013). Nitric oxide-releasing silica nanoparticle-doped polyurethane electrospun fibers. *ACS Applied Materials & Interfaces*, *5*(16), 7956–7964.

Liu, X., Lin, T., Gao, Y., Xu, Z., Huang, C., Yao, G., et al. (2012). Antimicrobial electrospun nanofibers of cellulose acetate and polyester urethane composite for wound dressing. *Journal of Biomedical Materials Research Part B: Applied Biomaterials*, *100B*(6), 1556–1565.

Locock, K. E. S., Michl, T. D., Valentin, J. D. P., Vasilev, K., Hayball, J. D., Qu, Y., et al. (2013). Guanylated polymethacrylates: A class of potent antimicrobial polymers with low hemolytic activity. *Biomacromolecules*, *14*(11), 4021–4031.

Mickova, A., Buzgo, M., Benada, O., Rampichova, M., Fisar, Z., Filova, E., et al. (2012). Core/shell nanofibers with embedded liposomes as a drug delivery system. *Biomacromolecules*, *13*(4), 952–962.

Mourtas, S., Fotopoulou, S., Duraj, S., Sfika, V., Tsakiroglou, C., & Antimisiaris, S. G. (2007). Liposomal drugs dispersed in hydrogels: Effect of liposome, drug and gel properties on drug release kinetics. *Colloids and Surfaces B: Biointerfaces*, *55*(2), 212–221.

Ohkawa, K., Minato, K. I., Kumagai, G., Hayashi, S., & Yamamoto, H. (2006). Chitosan nanofiber. *Biomacromolecules*, *7*(11), 3291–3294.

Peppas, N. A., & Sahlin, J. J. (1989). A simple equation for the description of solute release. III. Coupling of diffusion and relaxation. *International Journal of Pharmaceutics*, *57*(2), 169–172.

Pjanovic, R., Boskovic-Vragolovic, N., Veljkovic-Giga, J., Garic-Grulovic, R., Pejanovic, S., & Bugarski, B. (2010). Diffusion of drugs from hydrogels and liposomes as drug carriers. *Journal of Chemical Technology and Biotechnology*, *85*(5), 693–698.

Puglia, C., Bonina, F., Rizza, L., Cortesi, R., Merlotti, E., Drechsler, M., et al. (2010). Evaluation of percutaneous absorption of naproxen from different liposomal formulations. *Journal of Pharmaceutical Sciences*, *99*(6), 2819–2829.

Qi, R., Guo, R., Shen, M., Cao, X., Zhang, L., Xu, J., et al. (2010). Electrospun poly(lactic-co-glycolic acid)/halloysite nanotube composite nanofibers for drug encapsulation and sustained release. *Journal of Materials Chemistry*, *20*(47), 10622–10629.

Quemeneur, F., Rinaudo, M., Maret, G., & Pepin-Donat, B. (2010). Decoration of lipid vesicles by polyelectrolytes: Mechanism and structure. *Soft Matter*, *6*(18), 4471–4481.

Ritger, P. L., & Peppas, N. A. (1987a). A simple equation for description of solute release I. Fickian and non-Fickian release from non-swellable devices in the form of slabs, spheres, cylinders or discs. *Journal of Controlled Release*, *5*(1), 23–36.

Ritger, P. L., & Peppas, N. A. (1987b). A simple equation for description of solute release II. Fickian and anomalous release from swellable devices. *Journal of Controlled Release*, *5*(1), 37–42.

Schiffman, J. D., & Schauer, C. L. (2008). A review: Electrospinning of biopolymer nanofibers and their applications. *Polymer Reviews*, *48*(2), 317–352.

Shao, S., Li, L., Yang, G., Li, J., Luo, C., Gong, T., et al. (2011). Controlled green tea polyphenols release from electrospun PCL/MWCNTs composite nanofibers. *International Journal of Pharmaceutics*, *421*(2), 310–320.

Song, B., Wu, C., & Chang, J. (2012). Dual drug release from electrospun poly(lactic-co-glycolic acid)/mesoporous silica nanoparticles composite mats with distinct release profiles. *Acta Biomaterialia*, *8*(5), 1901–1907.

Todd, P. A., & Clissold, S. P. (1990). Naproxen – A reappraisal of its pharmacology, and therapeutic use in rheumatic diseases and pain states. *Drugs*, *40*(1), 91–137.

Tungprapa, S., Jangchud, I., & Supaphol, P. (2007). Release characteristics of four model drugs from drug-loaded electrospun cellulose acetate fiber mats. *Polymer*, *48*(17), 5030–5041.

Xie, Z., Paras, C. B., Weng, H., Punnakitikashem, P., Su, L. C., Vu, K., et al. (2013). Dual growth factor releasing multi-functional nanofibers for wound healing. *Acta Biomaterialia*, *9*(12), 9351–9359.

Yu, D.-G., Yang, J.-M., Li, L., Lu, P., & Zhu, L.-M. (2012). Comparison of two electrospinning processes in obtaining finer polymer nanofibers. *Fibers and Polymers*, *13*(4), 450–455.

Yu, D.-G., Yu, J.-H., Chen, L., Williams, G. R., & Wang, X. (2012). Modified coaxial electrospinning for the preparation of high-quality ketoprofen-loaded cellulose acetate nanofibers. *Carbohydrate Polymers*, *90*(2), 1016–1023.

Zahedi, P., Rezaeian, I., Ranaei-Siadat, S. O., Jafari, S. H., & Supaphol, P. (2010). A review on wound dressings with an emphasis on electrospun nanofibrous polymeric bandages. *Polymers for Advanced Technologies*, *21*(2), 77–95.

Zhang, D., & Chang, J. (2008). Electrospinning of three-dimensional nanofibrous tubes with controllable architectures. *Nano Letters*, *8*(10), 3283–3287.